

# DR-LoRA: Dynamic Rank LoRA for Mixture-of-Experts Adaptation

Guanzhi Deng<sup>1\*</sup>, Bo Li<sup>2\*</sup>, Ronghao Chen<sup>3\*</sup>, Huacan Wang<sup>4</sup>, Linqi Song<sup>1†</sup>, Lijie Wen<sup>2†</sup>

<sup>1</sup>City University of Hong Kong, Hong Kong, China

<sup>2</sup>Tsinghua University, Beijing, China

<sup>3</sup>Peking University, Beijing, China

<sup>4</sup>University of Chinese Academy of Sciences, Beijing, China

guanzdeng2-c@my.cityu.edu.hk, linqi.song@cityu.edu.hk

## Abstract

Mixture-of-Experts (MoE) has become a prominent paradigm for scaling Large Language Models (LLMs). Parameter-efficient fine-tuning (PEFT), such as LoRA, is widely adopted to adapt pretrained MoE LLMs to downstream tasks. However, existing approaches assign identical LoRA ranks to all experts, overlooking the intrinsic functional specialization within MoE LLMs. This uniform allocation leads to resource mismatch, task-relevant experts are under-provisioned while less relevant ones receive redundant parameters. We propose a Dynamic Rank LoRA framework named **DR-LoRA**, which dynamically grows expert LoRA ranks during fine-tuning based on task-specific demands. DR-LoRA employs an Expert Saliency Scoring mechanism that integrates expert routing frequency and LoRA rank importance to quantify each expert’s demand for additional capacity. Experts with higher saliency scores are prioritized for rank expansion, enabling the automatic formation of a heterogeneous rank distribution tailored to the target task. Experiments on multiple benchmarks demonstrate that DR-LoRA consistently outperforms standard LoRA and static allocation strategies under the same parameter budget, achieving superior task performance with more efficient parameter utilization.

## 1 Introduction

Mixture-of-Experts (MoE) has become a prominent paradigm for scaling Large Language Models (LLMs) (Yang et al., 2025; Jiang et al., 2024; Liu et al., 2024a). By sparsely activating only a subset of expert sub-networks for each input token, MoE substantially increases model capacity without proportionally increasing per-token computation, demonstrating impressive capabilities across a wide range of tasks (Shazeer et al., 2017; Fedus

et al., 2022; Jiang et al., 2024; Team et al., 2025).

With the widespread adoption of pretrained MoE LLMs, efficiently adapting them to specific downstream tasks has become a significant challenge.

Parameter-Efficient Fine-Tuning (PEFT), particularly Low-Rank Adaptation (LoRA) (Hu et al., 2022), is a primary approach to address this challenge. LoRA injects trainable low-rank matrices into pretrained models, enabling effective task adaptation with a small number of trainable parameters. However, existing approaches that apply LoRA to MoE are largely architecture-agnostic and treat all experts homogeneously. Specifically, they typically assign the same fixed LoRA rank to every expert (Li et al., 2024; Liu et al., 2024b; Dou et al., 2024; Gao et al., 2025). While simple, this strategy fundamentally overlooks the intrinsic functional specialization formed during MoE pretraining.

Recent studies have demonstrated that experts in pretrained MoE LLMs exhibit significant heterogeneity in their learned representations and functional roles, with different experts naturally developing specialization toward distinct knowledge domains, linguistic phenomena, or reasoning patterns (Wang et al., 2025; Fedus et al., 2022; Jiang et al., 2024). This intrinsic expert specialization constitutes the foundation of MoE’s powerful representational capacity. Under a uniform and fixed-rank LoRA configuration, experts that are highly relevant to the target domain may become under-provisioned due to insufficient adaptation capacity, while less relevant experts may be over-provisioned with redundant parameters. This resource mismatch limits the model’s adaptation potential and ultimately constrains its performance on downstream tasks.

While prior work has explored static heterogeneous expert designs for pre-training (Sun et al., 2024; Wang et al., 2025) and adaptive rank allocation for dense LLMs (Zhang et al., 2023), these studies do not address the challenge of dynamically

\*Equal contribution.

†Corresponding authors.

constructing task-specific, heterogeneous adaptation structures during the fine-tuning of existing pretrained MoE models. Existing work on PEFT for MoE models includes ESFT (Wang et al., 2024), which fine-tunes a fixed subset of experts, and PERFT (Liu et al., 2024d), which uses a uniform-rank LoRA configuration across experts. These designs restrict adaptation to coarse-grained or homogeneous capacity allocation, preventing fine-grained and dynamic expert-level adaptation during training.

To address this issue, we propose a Dynamic Rank LoRA framework named **DR-LoRA**, which enables expert adaptation capacity to evolve dynamically in response to task-specific demands during fine-tuning. Unlike uniform allocation strategies, DR-LoRA adopts an incremental growth approach: it allocates high-rank LoRA parameter space to each expert at initialization but activates only a small initial rank, then progressively expands the effective rank of high-demand experts throughout training. This expansion is guided by an Expert Saliency Scoring mechanism that integrates two complementary signals from the MoE training process: (1) expert routing frequency, tracked via exponential moving average of routing weights, which quantifies each expert’s relevance to the current data distribution (Zhou et al., 2022); and (2) LoRA rank importance, measured through accumulated gradient-weight products, which captures the learning intensity of each expert on the target task (Zhang et al., 2023). By computing the saliency, DR-LoRA prioritizes rank allocation to experts with high task relevance and learning activity, while the rank penalty term prevents resource monopolization and promotes balanced capacity distribution.

The contributions of this paper are summarized as follows:

- We identify the resource mismatch problem of uniform LoRA allocation in MoE adaptation, where task-relevant experts are under-provisioned while less relevant ones receive redundant parameters.
- We propose DR-LoRA, which dynamically grows LoRA ranks through an Expert Saliency Scoring mechanism that integrates routing frequency and rank importance, automatically forming task-adaptive heterogeneous rank distributions.

- Experiments demonstrate that DR-LoRA consistently outperforms standard LoRA and pruning-based methods under the same parameter budget, with analyses confirming effective task-aligned capacity allocation.

## 2 Related Work

Efficiently adapting LLMs to downstream tasks under resource constraints is a significant challenge, where Low-Rank Adaptation (LoRA) has emerged as a widely adopted Parameter-Efficient Fine-Tuning (PEFT) method.

Standard LoRA (Liu et al., 2024c; Hayou et al., 2024) assigns fixed and identical ranks to all target modules, but this overlooks the varying contributions of different modules to downstream tasks. To address this issue, researchers have proposed various dynamic rank allocation methods. AdaLoRA (Zhang et al., 2023) parameterizes weight updates in singular value decomposition form and adaptively adjusts the rank of each module during training through importance score-based pruning. However, this high-to-low pruning strategy incurs substantial computational overhead in the early stages of training. Although these methods have advanced adaptive PEFT for dense LLMs, they do not consider the unique characteristics of MoE LLMs, particularly the special challenges posed by expert heterogeneity.

Experts in MoE LLMs are known to form functional specializations after pre-training (Dai et al., 2024). This intrinsic heterogeneity presents a special challenge for PEFT, as a uniform adaptation strategy fails to match the non-uniform functional distribution of the experts. Existing work on PEFT for MoE models includes ESFT (Wang et al., 2024), which fine-tunes a fixed subset of experts, and PERFT (Liu et al., 2024d), which uses a uniform-rank LoRA configuration across experts. These designs restrict adaptation to coarse-grained or homogeneous capacity allocation, preventing fine-grained and dynamic expert-level adaptation during training.

In this work, we propose DR-LoRA, which exploits expert heterogeneity for dynamic rank allocation. By continuously assessing each expert’s routing frequency and learning intensity during training, DR-LoRA incrementally grows LoRA ranks to construct task-adaptive heterogeneous distributions, outperforming uniform and pruning-based allocation strategies.

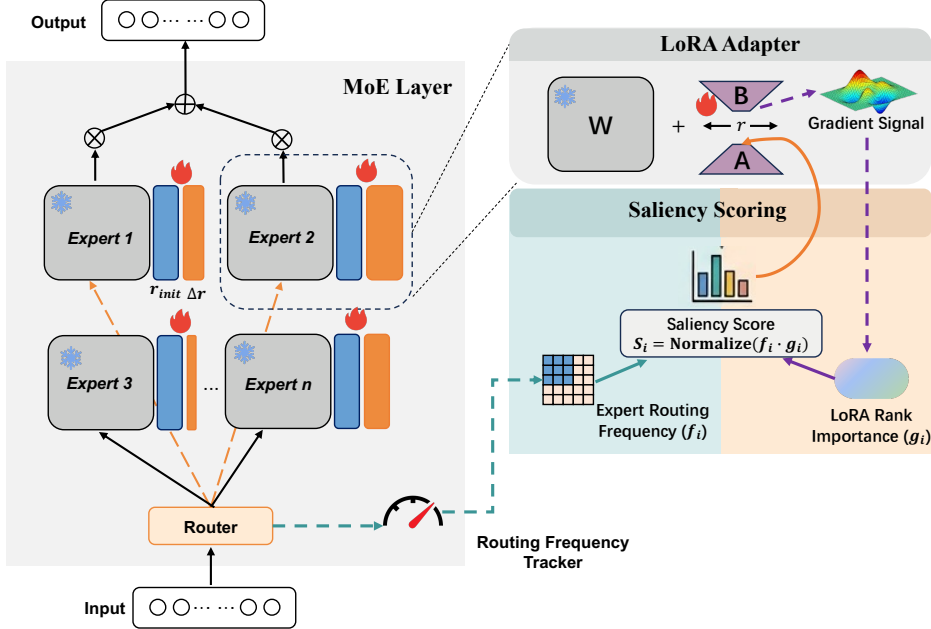


Figure 1: The overview of the DR-LoRA framework. Pre-trained expert weights are frozen, while each expert is equipped with a trainable LoRA module. These modules start with a small initial rank ( $r_{\text{init}}$ ) and can dynamically grow ( $\Delta r$ ) during training. Expert Saliency Scoring guides rank growth by integrating two real-time signals: (1) **Expert Routing Frequency** ( $f_i$ ), tracked from the router’s decisions to measure task relevance, and (2) **LoRA Rank Importance** ( $g_i$ ), derived from the gradient signals of the trainable LoRA matrices (A and B) to measure learning intensity.

### 3 Methodology

In this section, we present DR-LoRA (Dynamic Rank LoRA), a framework that dynamically adapts LoRA ranks during fine-tuning to address the resource mismatch problem in MoE adaptation. As shown in Figure 1, we first formulate the problem setup (§3.1), then introduce our core Expert Saliency Scoring mechanism (§3.2), and finally present the dynamic rank allocation strategy (§3.3).

#### 3.1 Problem Formulation

**MoE Architecture.** We consider a standard Mixture-of-Experts LLM with  $L$  transformer layers. For each layer  $\ell \in \{1, \dots, L\}$ , the MoE module contains  $N$  expert networks  $\{E_{\ell,1}, \dots, E_{\ell,N}\}$  and a router  $G_\ell$  that produces routing weights. For an input token representation  $\mathbf{x}_\ell$ , the router computes:

$$\mathbf{w}_\ell = \text{Softmax}(G_\ell(\mathbf{x}_\ell)) \in \mathbb{R}^N \quad (1)$$

In top- $k$  routing, only the top- $k$  experts with the highest routing weights are activated. The MoE output is:

$$\text{MoE}_\ell(\mathbf{x}_\ell) = \sum_{i \in \text{TopK}(\mathbf{w}_\ell)} w_{\ell,i} \cdot E_{\ell,i}(\mathbf{x}_\ell) \quad (2)$$

**LoRA Adaptation.** Following [Hu et al. \(2022\)](#), LoRA adapts a pretrained weight matrix  $\mathbf{W} \in \mathbb{R}^{d \times k}$  by injecting trainable low-rank matrices:

$$\mathbf{W}' = \mathbf{W} + \mathbf{B}\mathbf{A} \quad (3)$$

where  $\mathbf{A} \in \mathbb{R}^{r \times k}$  and  $\mathbf{B} \in \mathbb{R}^{d \times r}$  with rank  $r \ll \min(d, k)$ . During training,  $\mathbf{W}$  is frozen while  $\mathbf{A}$  and  $\mathbf{B}$  are updated.

Existing LoRA methods for MoE assign uniform rank  $r$  to all experts. However, experts in pretrained MoE models exhibit significant functional specialization ([Dai et al., 2024](#); [Muennighoff et al., 2025](#)), with different experts naturally suited for different aspects of the data distribution. During task-specific fine-tuning, this specialization creates varying adaptation demands: task-relevant experts require substantial capacity to fully leverage their specialization, while task-irrelevant experts need minimal updates primarily for distributional alignment. Uniform allocation thus leads to under-provisioning of critical experts and over-provisioning of less relevant ones, resulting in sub-optimal parameter utilization and limited adaptation quality.

We aim to construct a heterogeneous rank distribution  $\{\mathcal{R}_{\ell,i}\}_{\ell,i}$  where each expert’s LoRA rank

$\mathcal{R}_{\ell,i}$  reflects its task-specific demand, while maintaining a fixed total parameter budget:

$$\sum_{\ell=1}^L \sum_{i=1}^N \mathcal{R}_{\ell,i} = L \times N \times r_{\text{target}} \quad (4)$$

where  $r_{\text{target}}$  is the target average rank equivalent to standard LoRA.

### 3.2 Expert Saliency Scoring

To quantify each expert’s demand for additional parameters, we propose an Expert Saliency Scoring mechanism that integrates two complementary signals from the MoE training process.

**Expert Routing Frequency.** The routing frequency reflects how often an expert is selected during training, which indicates its relevance to the current data distribution. For expert  $\mathcal{E}_{\ell,i}$  at layer  $\ell$ , we track its usage via an exponential moving average (EMA):

$$f_{\ell,i}^{(t)} = \beta \cdot f_{\ell,i}^{(t-1)} + (1 - \beta) \cdot w_{\ell,i}^{(t)} \quad (5)$$

where  $w_{\ell,i}^{(t)}$  is the weight of tokens routed to expert  $\mathcal{E}_{\ell,i}$  at step  $t$ , and  $\beta \in [0, 1)$  is the decay coefficient.

**LoRA Rank Importance.** The rank importance measures the learning intensity of an expert, reflecting how actively it is adapting to the current task. Following Zhang et al. (2023), we employ a sensitivity-based importance metric that measures each rank dimension’s contribution through gradient-weight products.

For each expert’s LoRA module, we denote  $\mathbf{a}_j = \mathbf{A}_{\ell,i}[j, :]$  and  $\mathbf{b}_j = \mathbf{B}_{\ell,i}[:, j]$  as the  $j$ -th rank dimension parameters. We compute the important score at step  $t$  as:

$$s_{\ell,i,j}^{(t)} = \left\| \frac{\partial \mathcal{L}}{\partial \mathbf{a}_j} \odot \mathbf{a}_j \right\|_1 \cdot \left\| \frac{\partial \mathcal{L}}{\partial \mathbf{b}_j} \odot \mathbf{b}_j \right\|_1 \quad (6)$$

where  $\mathcal{L}$  is the training loss,  $\odot$  denotes element-wise product, and  $\|\cdot\|_1$  denotes the  $\ell_1$  norm. We employ multiplicative aggregation to reflect the joint contribution of LoRA’s doublet  $\{\mathbf{a}_j, \mathbf{b}_j\}$ .

We then track the rank importance using the same EMA coefficient:

$$g_{\ell,i,j}^{(t)} = \beta \cdot g_{\ell,i,j}^{(t-1)} + (1 - \beta) \cdot s_{\ell,i,j}^{(t)} \quad (7)$$

The expert-level rank importance aggregates over active ranks:

$$g_{\ell,i}^{(t)} = \frac{1}{r_{\ell,i}^{(t)}} \sum_{j=1}^{r_{\ell,i}^{(t)}} g_{\ell,i,j}^{(t)} \quad (8)$$

**Saliency Score.** We define **saliency score** as follows:

$$\mathcal{S}_{\ell,i}^{(t)} = \frac{f_{\ell,i}^{(t)} \cdot g_{\ell,i}^{(t)}}{(r_{\ell,i}^{(t)} + 1)^\gamma} \quad (9)$$

We integrate routing frequency and rank importance as complementary signals to quantify each expert’s demand for additional capacity. The rank penalty term  $(r_{\ell,i}^{(t)} + 1)^{-\gamma}$  prevents individual experts from monopolizing resources and promotes a balanced rank distribution.

### 3.3 Dynamic Rank Allocation Strategy

DR-LoRA adopts an incremental rank expansion strategy during supervised fine-tuning. We initialize all experts with a small active rank and progressively activate additional rank dimensions for high-saliency experts, guided by the Expert Saliency Scoring mechanism described in §3.2.

**Initialization.** At the start of training, each expert  $E_{\ell,i}$  allocates parameter space for  $r_{\text{max}}$  ranks by initializing  $\mathbf{A}_{\ell,i} \in \mathbb{R}^{r_{\text{max}} \times k}$  and  $\mathbf{B}_{\ell,i} \in \mathbb{R}^{d \times r_{\text{max}}}$ , but only activates the first  $r_{\text{init}}$  dimensions. A binary mask  $\mathbf{m}_{\ell,i} \in \{0, 1\}^{r_{\text{max}}}$  tracks active dimensions, with the forward pass computing:

$$\mathbf{W}'_{\ell,i} = \mathbf{W}_{\ell,i} + \mathbf{B}_{\ell,i}[:, \mathbf{m}_{\ell,i}] \cdot \mathbf{A}_{\ell,i}[\mathbf{m}_{\ell,i}, :] \quad (10)$$

**Growth Window and Budget Allocation.** We define a growth window  $[t_{\text{warmup}}, t_{\text{end}}]$  during which rank expansion occurs, where  $t_{\text{warmup}}$  is the learning rate warmup period,  $t_{\text{end}} = T_{\text{total}} - T_{\text{buffer}}$ , and  $T_{\text{buffer}}$  ensures newly activated ranks have sufficient training time. Within this window, we perform rank growth every  $T_{\text{grow}}$  steps.

To ensure balanced growth across the training period, we pre-compute a fixed quota  $Q$  for each growth event. First, we compute the total number of growth events:  $T_{\text{events}} = \lfloor (t_{\text{end}} - t_{\text{warmup}}) / T_{\text{grow}} \rfloor$ . Then, the quota is determined as:

$$Q = \left\lceil \frac{N \times (r_{\text{target}} - r_{\text{init}})}{T_{\text{events}}} \right\rceil \quad (11)$$

This quota represents the number of ranks to distribute per layer at each growth event, ensuring that the total active ranks reach  $N \times r_{\text{target}}$  by the end of the growth window.

**Periodic Rank Growth.** Every  $T_{\text{grow}}$  steps within the growth window, we execute a rank allocation procedure for each layer independently based on expert saliency scores. For each layer

---

**Algorithm 1** DR-LoRA Training Algorithm

---

**Require:** Pretrained MoE model ( $L$  layers,  $N$  experts/layer), dataset  $\mathcal{D}$ , hyperparameters  $\{r_{\text{init}}, r_{\text{max}}, r_{\text{target}}, T_{\text{grow}}, p_{\text{grow}}, \beta, \gamma\}$

**Ensure:** Fine-tuned model with heterogeneous expert ranks

- 1: **Initialize:** Allocate  $\mathbf{A}_{\ell,i} \in \mathbb{R}^{r_{\text{max}} \times k}$ ,  $\mathbf{B}_{\ell,i} \in \mathbb{R}^{d \times r_{\text{max}}}$  with masks  $\mathbf{m}_{\ell,i}$ ; Freeze router; Compute quota  $Q$  (Eq. 11)
- 2: **for**  $t = 1$  to  $T_{\text{total}}$  **do**
- 3:   Sample batch  $\mathcal{B}$ ; Compute MoE output and loss  $\mathcal{L}(\mathcal{B})$
- 4:   Update routing frequency  $f_{\ell,i}^{(t)}$  (Eq. 5) and gradient score  $g_{\ell,i}^{(t)}$  (Eq. 8)
- 5:   **if**  $t = t_{\text{warmup}}$  **then**
- 6:     Unfreeze router
- 7:   **end if**
- 8:   **if**  $t \in [t_{\text{warmup}}, t_{\text{end}}]$  **and**  $(t - t_{\text{warmup}}) \bmod T_{\text{grow}} = 0$  **then**
- 9:     **for** each layer  $\ell$  **do**
- 10:       Compute saliency  $S_{\ell,i}^{(t)}$  (Eq. 9)
- 11:       Sort experts
- 12:       Allocate  $Q$  ranks greedily: for each expert  $i$  in order, activate  $n_{\text{grow}}$  (Eq. 12) ranks
- 13:       Reset  $g_{\ell,i}$  for all experts
- 14:     **end for**
- 15:   **end if**
- 16:   Update  $\mathbf{A}_{\ell,i}$ ,  $\mathbf{B}_{\ell,i}$  and router
- 17: **end for**

---

$\ell$ , we first compute the saliency score  $S_{\ell,i}^{(t)}$  for all experts using Eq.(9), then sort the experts in descending order of their scores. We then perform greedy allocation of the pre-computed quota  $Q$  to high-saliency experts. Specifically, for each expert  $i$  in the sorted order, we determine the number of new ranks to allocate as:

$$n_{\text{grow}} = \min(\lfloor r_{\text{free}} \times p_{\text{grow}} \rfloor, r_{\text{avail},i}, Q_{\text{remain}}) \quad (12)$$

where  $r_{\text{free}} = r_{\text{max}} - r_{\text{init}}$  is the initial free capacity,  $r_{\text{avail},i}$  is the current number of inactive ranks, and  $p_{\text{grow}}$  is the maximum growth rate per expert per event that prevents any single expert from monopolizing the quota in one growth event.

After allocating  $n_{\text{grow}}$  ranks to expert  $i$  by activating the corresponding dimensions in the mask  $\mathbf{m}_{\ell,i}$ , we reset its rank importance score  $g_{\ell,i} = 0$  while preserving its routing frequency  $f_{\ell,i}$ . Resetting rank importance scores prevents monopolization

and allows other experts to compete for ranks in subsequent allocations, while preserving routing frequency enables experts that have received ranks to remain competitive for future allocations as task demands evolve during training.

The complete training procedure integrating this growth strategy is presented in Algorithm 1.

## 4 Experiments

### 4.1 Experimental Setup

**Datasets.** We employ the OLMoE SFT Mix dataset<sup>1</sup>, a comprehensive mixture of instruction-following, mathematical reasoning, and coding samples.

**Models and Baselines.** We evaluate DR-LoRA on two MoE architectures: **OLMoE-1B-7B-0924** (Muennighoff et al., 2025, hereafter OLMoE): 6.9B parameters (1.3B activated), 16 layers with 64 experts per layer, top-8 routing. **Phi-mini-MoE-instruct** (Abdin et al., 2024, hereafter Phi): 7.6B parameters (2.4B activated), 32 layers with 16 experts per layer, top-2 routing.

We compare against: (1) **Base Model**: Pre-trained model without fine-tuning; (2) **LoRA**: Uniform rank  $r = 64$  (OLMoE) /  $r = 16$  (Phi); (3) **DoRA**: Weight-decomposed adaptation (Liu et al., 2024c) with uniform rank  $r = 64$  /  $r = 16$ ; (4) **LoRA+**: Different learning rates for adapter matrices ( $\lambda = 16$ ) (Hayou et al., 2024) with uniform rank  $r = 64$  /  $r = 16$ ; (5) **AdaLoRA**: Adaptive pruning from  $r = 128$  to  $r = 64$  (OLMoE) /  $r = 32$  to  $r = 16$  (Phi) (Zhang et al., 2023); (6) **DR-LoRA**: Dynamic growth from  $r_{\text{init}} = 32$  to  $r_{\text{target}} = 64$  (OLMoE) /  $r_{\text{init}} = 8$  to  $r_{\text{target}} = 16$  (Phi).

**Training Configuration.** All models train for one epoch with the same parameter budget. We apply LoRA to up\_proj and down\_proj matrices. For AdaLoRA and DR-LoRA, rank updates occur every 200 steps. Details in Appendix A.1.

**Evaluation.** We evaluate on seven benchmarks: MMLU (Hendrycks et al., 2020), HellaSwag (Zellers et al., 2019), BBH (Suzgun et al., 2023), GSM8k (Cobbe et al., 2021), ARC-C (Clark et al., 2018), HumanEval (Chen, 2021), and IFEval (Zhou et al., 2023), covering knowledge, reasoning, code generation, and instruction following.

<sup>1</sup><https://huggingface.co/datasets/allenai/tulu-v3.1-mix-preview-4096-OLMoE>

Model	Eff. Rank	MMLU	HellaSwag	BBH	GSM8k	ARC-C	HumanEval	IFEval	Avg
<i>OLMoE Models</i>									
Base	–	<u>50.5</u>	<b>59.2</b>	32.3	6.1	<b>54.2</b>	22.1	16.5	34.4
LoRA	64	50.3	55.9	<b>34.5</b>	30.2	51.9	34.1	28.8	40.8
DoRA	64	50.4	56.1	34.2	30.9	52.1	35.3	29.2	41.2
LoRA+	64	<b>50.6</b>	<u>56.3</u>	<u>34.4</u>	31.2	52.4	36.2	<u>29.8</u>	<u>41.6</u>
AdaLoRA	128→64	<b>50.6</b>	55.8	33.3	<u>31.6</u>	52.2	<u>37.5</u>	29.5	41.5
DR-LoRA	32→64	50.0	55.9	<b>34.5</b>	<b>32.8</b>	<u>53.2</u>	<b>39.1</b>	<b>32.7</b>	<b>42.6</b>
<i>Phi Models</i>									
Base	–	<b>67.6</b>	54.6	48.7	71.3	58.4	72.3	47.3	60.0
LoRA	16	67.2	54.7	68.1	75.0	<b>58.8</b>	79.8	47.9	64.5
DoRA	16	67.3	55.1	68.5	76.2	58.6	80.7	48.4	64.9
LoRA+	16	<u>67.5</u>	55.4	68.8	<u>77.1</u>	<u>58.7</u>	81.5	49.1	65.4
AdaLoRA	32→16	67.4	<u>55.7</u>	<u>69.0</u>	76.8	<u>58.7</u>	<u>82.2</u>	48.8	<u>65.5</u>
DR-LoRA	8→16	<b>67.6</b>	<b>56.9</b>	<b>69.9</b>	<b>78.2</b>	58.4	<b>84.6</b>	<b>49.5</b>	<b>66.4</b>

Table 1: Benchmark performance of fine-tuned models across different MoE architectures. **Bold** indicates best performance; underline indicates second-best. All methods maintain the same parameter budget ( $r_{avg} = 64$  for OLMoE,  $r_{avg} = 16$  for Phi).

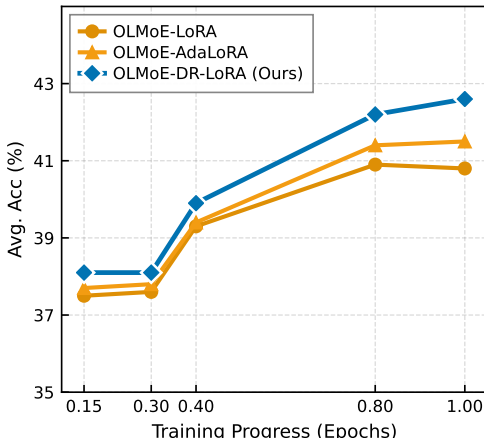


Figure 2: Average accuracy on task-aligned benchmarks (GSM8k, HumanEval, IFEval) during training. DR-LoRA establishes early superiority and maintains the advantage throughout training.

We track performance throughout training at 6000-step intervals.

## 4.2 Main Results

**Overall Performance.** Table 1 presents the benchmark results at the end of training:

(1) **Strong task adaptation:** DR-LoRA demonstrates significant improvements on benchmarks aligned with training emphasis. On OLMoE, DR-LoRA outperforms LoRA by +2.6 points on GSM8k (math reasoning), +5.0 on HumanEval (code generation), and +3.9 on IFEval (instruction-following). Compared to the task-

specific second-best method, DR-LoRA achieves gains of +1.2, +1.6, and +2.9 points respectively on these tasks. On Phi, DR-LoRA achieves +3.2, +4.8, and +1.6 improvements over LoRA on the same benchmarks, and +1.1, +2.4, and +0.4 over the task-specific second-best baseline.

(2) **Robust general performance:** DR-LoRA achieves the best overall performance, with average improvements of +1.8 points over LoRA on OLMoE and +1.9 points on Phi. Beyond task-aligned benchmarks, DR-LoRA maintains strong capabilities on general knowledge tasks (MMLU, HellaSwag, ARC-C). On Phi, DR-LoRA improves +2.2 points over LoRA on HellaSwag while matching the pretrained model’s performance on MMLU.

(3) **Growth beats pruning:** DR-LoRA’s incremental allocation strategy outperforms the pruning-based AdaLoRA approach by +1.1 average points on OLMoE and +0.9 points on Phi. This suggests that gradually allocating capacity to high-demand experts is more effective than pruning from over-provisioned initialization.

**Training Dynamics.** To understand the learning behavior, we track OLMoE’s performance throughout training, averaged across GSM8k, HumanEval, and IFEval (Figure 2). DR-LoRA demonstrates early superiority and maintains its advantage throughout training, suggesting it rapidly identifies and prioritizes task-relevant experts while uniform LoRA spreads limited learning capacity across all experts equally.

Model Variant	GSM8k	HE	IF	Avg
w/o Routing Freq.	31.4	38.0	30.3	33.2
w/o Rank Imp.	32.1	37.8	29.9	33.3
<b>Full DR-LoRA</b>	<b>32.8</b>	<b>39.1</b>	<b>32.7</b>	<b>34.9</b>

Table 2: Ablation of saliency score components. Both routing frequency and rank importance contribute meaningfully to overall performance.

Configuration	GSM8k	HE	IF	Avg
Router Frozen	31.6	36.7	29.7	32.7
<b>Router Unfrozen</b>	<b>32.8</b>	<b>39.1</b>	<b>32.7</b>	<b>34.9</b>

Table 3: Impact of router freezing. Unfreezing the router after warmup yields better results, enabling adaptive routing to evolved expert capabilities.

### 4.3 Ablation Study

To validate each component in our saliency scoring mechanism, we evaluate three configurations: (1) Full DR-LoRA with both routing frequency and rank importance; (2) w/o Routing Frequency, using only rank importance ( $g_{\ell,i}$ ); (3) w/o Rank Importance, using only routing frequency ( $f_{\ell,i}$ ).

Table 2 shows that full DR-LoRA consistently outperforms both ablated variants (+1.7 average points), confirming both components are necessary. To understand their distinct contributions, we compare the top-25% highest-ranked experts (16 out of 64 experts per layer) across configurations.

Figure 7 in Appendix reveals that despite moderate overlap (74.6% and 84.8%), the ablated variants allocate high ranks to 65 and 39 different experts respectively, indicating that each component captures non-redundant information. This validates that the multiplicative saliency function (Eq. 9) effectively integrates complementary signals, data relevance ( $f_{\ell,i}$ ) and learning dynamics ( $g_{\ell,i}$ ), for optimal rank allocation.

We compare freezing versus unfreezing the MoE router during fine-tuning. Table 3 shows that unfreezing the router after warmup improves performance (+2.2 average points), enabling adaptive routing to exploit evolved expert capabilities from heterogeneous rank allocation. All experiments unfreeze the router unless specified.

## 5 Analysis

### 5.1 Expert-Task Alignment Analysis

To verify that DR-LoRA indeed allocates more parameters to task-relevant experts, we conduct a masking experiment by selectively disabling expert

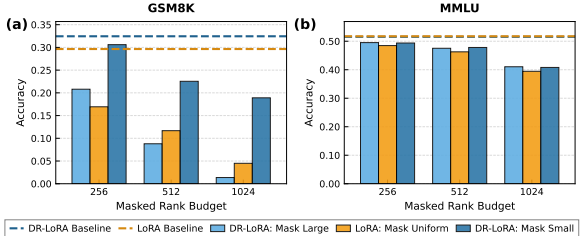


Figure 3: Performance degradation when masking expert subgroups. On math tasks (GSM8k), masking large experts causes  $4\times$  greater degradation than masking small experts, confirming task-aligned capacity allocation. On general knowledge (MMLU), both groups contribute similarly.

subsets based on their final ranks and measuring the resulting performance degradation.

We partition experts into large experts (top-25% by rank) and small experts (remaining 75%). For each model, we randomly mask experts from each group and evaluate the impact. We mask *entire* experts modules (including both pretrained weight matrices and LoRA modules), not just LoRA components.

We experiment with three masking budgets: 256, 512, and 1024 ranks per layer (approximately 6%, 12%, and 25% of the 4096 total ranks per layer). Due to DR-LoRA’s heterogeneous rank distribution, the same rank budget translates to different numbers of masked experts: masking 256 ranks disable  $\sim 2$  large experts (each with  $r \approx 128$ ) but  $\sim 4$  small experts (each with  $r \approx 64$ ).

As shown in Figure 3, key findings emerge:

(1) *Disproportionate importance on aligned tasks*: On GSM8k, masking large DR-LoRA experts causes substantially larger performance drops than masking small experts across all budgets, confirming DR-LoRA concentrates critical mathematical reasoning capacity in high-rank experts.

(2) *Uniform distribution on non-aligned tasks*: On MMLU, masking large vs. small experts yields comparable degradation, indicating general knowledge remains uniformly distributed across experts.

Notably, since LoRA parameters are negligible compared to expert parameters, masking small experts actually removes *more* total parameters. The disproportionate performance impact of large experts despite their smaller parameter footprint demonstrates **effective capacity allocation**: DR-LoRA invests minimal parameters in task-critical experts to achieve maximal performance gains.

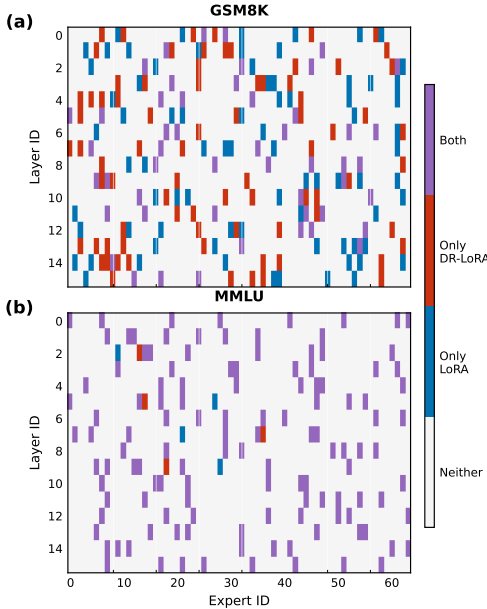


Figure 4: Expert activation heatmaps on different tasks. On GSM8k, DR-LoRA and LoRA exhibit distinctly different activation patterns. On MMLU, both methods activate largely overlapping expert sets.

## 5.2 Expert Activation Patterns

We track the most frequently activated experts (top-8 by routing frequency) for both DR-LoRA and standard LoRA when evaluating on GSM8k and MMLU. Figure 4 reveals that on GSM8k, DR-LoRA and LoRA activate largely different expert sets, while on MMLU, both methods show substantial overlap. This divergence on GSM8k confirms that DR-LoRA identifies and amplifies task-relevant experts during training: by allocating more ranks to math-capable experts, DR-LoRA enables them to fully develop their specialization, while uniform LoRA’s equal allocation prevents such targeted enhancement, resulting in fundamentally different expert utilization patterns.

## 5.3 Impact of Growth Interval

We examine rank allocation intervals of 100, 200, and 500 steps. Table 4 shows all three frequencies substantially outperform standard LoRA (+1.1 to +2.2 average points), demonstrating robustness across growth schedules.

More frequent updates allow faster adaptation to emerging task demands but may introduce instability during early training. Less frequent updates provide more stable training but may respond slowly to changing expert requirements. The 200-step interval achieves the best balance, providing sufficient time for importance scores to stabilize while re-

Model	GSM8k	HE	IF	Avg
Base Model	6.1	22.1	16.5	14.9
OLMoE-LoRA	30.2	34.1	28.8	31.0
DR-LoRA (100s)	32.4	38.5	29.8	33.6
<b>DR-LoRA (200s)</b>	<b>32.8</b>	<b>39.1</b>	<b>32.7</b>	<b>34.9</b>
DR-LoRA (500s)	32.1	37.1	30.1	33.1

Table 4: Impact of rank growth interval. All three frequencies substantially outperform standard LoRA, with 200-step interval performing best.

Model	MedQA	MedMCQA	PubMed	Weighted Avg
Base	31.2	21.8	37.6	29.0
LoRA	43.6	31.5	46.0	40.4
<b>DR-LoRA</b>	<b>46.0</b>	<b>35.8</b>	<b>64.8</b>	<b>44.4</b>

Table 5: Generality of DR-LoRA on domain-specific adaptation. We fine-tune  $\Phi$  on medical QA datasets. DR-LoRA consistently outperforms standard LoRA across all medical benchmarks.

maining responsive to task-specific patterns. Based on these results, all experiments use 200-step intervals unless otherwise specified.

## 5.4 Domain Adaptation

To evaluate DR-LoRA’s effectiveness on domain-specific adaptation, we fine-tune  $\Phi$  on medical QA datasets. Detailed experimental configurations are provided in Appendix A.2. As shown in Table 5, DR-LoRA consistently outperforms standard LoRA across all benchmarks (+4.0 average points), with particularly strong gains on PubMedQA (+18.8 points). This demonstrates that DR-LoRA’s dynamic rank allocation successfully generalizes to domain-specific tasks beyond general instruction following.

## 6 Conclusion

In this work, we address the resource mismatch problem in MoE adaptation where uniform LoRA rank allocation fails to account for expert functional specialization. We propose DR-LoRA, a dynamic rank allocation framework that progressively grows expert LoRA ranks through an Expert Saliency Scoring mechanism integrating routing frequency and rank importance. Extensive experiments demonstrate that DR-LoRA consistently outperforms standard LoRA and pruning-based methods under the same parameter budget, effectively allocating capacity to task-relevant experts while maintaining robust general capabilities across different MoE architectures and tasks.

## Limitation

Although DR-LoRA demonstrate consistent improvements over existing methods, several limitations warrant discussion: (I) This study primarily validates the effectiveness of DR-LoRA in MoE LLMs that use a top-k routing mechanism. Our Expert Saliency Scoring mechanism is based on routing frequency, but the effectiveness of this metric has yet to be verified in architectures with different routing strategies, such as Expert Choice Routing, or in other domains like multimodal MoE LLMs. (II) While our experiments demonstrate the method’s generalizability across several models of varying scales and architectures, its scalability to much larger MoE models (e.g., those in the 100B+ parameter class) has not been explored. Therefore, extending the principles of DR-LoRA to more diverse MoE architectures and larger-scale models is an important direction for future work.

## Ethics Statement

This study adheres to the ethical guidelines set forth by our institution and follows the principles outlined in the ACM Code of Ethics and Professional Conduct. All datasets used in our experiments are publicly available.

## References

Marah Abdin, Jyoti Aneja, Harkirat Behl, Sébastien Bubeck, Ronen Eldan, Suriya Gunasekar, Michael Harrison, Russell J Hewett, Mojan Javaheripi, Piero Kauffmann, and 1 others. 2024. Phi-4 technical report. *arXiv preprint arXiv:2412.08905*.

Mark Chen. 2021. Evaluating large language models trained on code. *arXiv preprint arXiv:2107.03374*.

Peter Clark, Isaac Cowhey, Oren Etzioni, Tushar Khot, Ashish Sabharwal, Carissa Schoenick, and Oyvind Tafjord. 2018. Think you have solved question answering? try arc, the ai2 reasoning challenge. *arXiv preprint arXiv:1803.05457*.

Karl Cobbe, Vineet Kosaraju, Mohammad Bavarian, Mark Chen, Heewoo Jun, Lukasz Kaiser, Matthias Plappert, Jerry Tworek, Jacob Hilton, Reiichiro Nakano, and 1 others. 2021. Training verifiers to solve math word problems. *arXiv preprint arXiv:2110.14168*.

Damai Dai, Chengqi Deng, Chenggang Zhao, RX Xu, Huazuo Gao, Deli Chen, Jiashi Li, Wangding Zeng, Xingkai Yu, Yu Wu, and 1 others. 2024. Deepseek-moe: Towards ultimate expert specialization in mixture-of-experts language models. *arXiv preprint arXiv:2401.06066*.

Shihan Dou, Enyu Zhou, Yan Liu, Songyang Gao, Wei Shen, Limao Xiong, Yuhao Zhou, Xiao Wang, Zhi-heng Xi, Xiaoran Fan, and 1 others. 2024. Loramoe: Alleviating world knowledge forgetting in large language models via moe-style plugin. In *Proceedings of the 62nd Annual Meeting of the Association for Computational Linguistics (Volume 1: Long Papers)*, pages 1932–1945.

William Fedus, Barret Zoph, and Noam Shazeer. 2022. Switch transformers: Scaling to trillion parameter models with simple and efficient sparsity. *Journal of Machine Learning Research*, 23(120):1–39.

Chongyang Gao, Kezhen Chen, Jinmeng Rao, Ruibo Liu, Baochen Sun, Yawen Zhang, Daiyi Peng, Xiaoyuan Guo, and VS Subrahmanian. 2025. Mola: Moe lora with layer-wise expert allocation. In *Findings of the Association for Computational Linguistics: NAACL 2025*, pages 5097–5112.

Soufiane Hayou, Nikhil Ghosh, and Bin Yu. 2024. Lora+: Efficient low rank adaptation of large models. *arXiv preprint arXiv:2402.12354*.

Dan Hendrycks, Collin Burns, Steven Basart, Andy Zou, Mantas Mazeika, Dawn Song, and Jacob Steinhardt. 2020. Measuring massive multitask language understanding. *arXiv preprint arXiv:2009.03300*.

Edward J Hu, yelong shen, Phillip Wallis, Zeyuan Allen-Zhu, Yuanzhi Li, Shean Wang, Lu Wang, and Weizhu Chen. 2022. LoRA: Low-rank adaptation of large language models. In *International Conference on Learning Representations*.

Albert Q Jiang, Alexandre Sablayrolles, Antoine Roux, Arthur Mensch, Blanche Savary, Chris Bamford, Devendra Singh Chaplot, Diego de las Casas, Emma Bou Hanna, Florian Bressand, and 1 others. 2024. Mixtral of experts. *arXiv preprint arXiv:2401.04088*.

Dengchun Li, Yingzi Ma, Naizheng Wang, Zheng-mao Ye, Zhiyuan Cheng, Yinghao Tang, Yan Zhang, Lei Duan, Jie Zuo, Cal Yang, and 1 others. 2024. Mixlora: Enhancing large language models finetuning with lora-based mixture of experts. *arXiv preprint arXiv:2404.15159*.

Aixin Liu, Bei Feng, Bing Xue, Bingxuan Wang, Bochao Wu, Chengda Lu, Chenggang Zhao, Chengqi Deng, Chenyu Zhang, Chong Ruan, and 1 others. 2024a. Deepseek-v3 technical report. *arXiv preprint arXiv:2412.19437*.

Qidong Liu, Xian Wu, Xiangyu Zhao, Yuanshao Zhu, Derong Xu, Feng Tian, and Yefeng Zheng. 2024b. When moe meets llms: Parameter efficient finetuning for multi-task medical applications. In *Proceedings of the 47th International ACM SIGIR Conference on Research and Development in Information Retrieval*, pages 1104–1114.

Shih-Yang Liu, Chien-Yi Wang, Hongxu Yin, Pavlo Molchanov, Yu-Chiang Frank Wang, Kwang-Ting

Cheng, and Min-Hung Chen. 2024c. Dora: Weight-decomposed low-rank adaptation. In *Forty-first International Conference on Machine Learning*.

Yilun Liu, Yunpu Ma, Shuo Chen, Zifeng Ding, Bailan He, Zhen Han, and Volker Tresp. 2024d. Perft: Parameter-efficient routed fine-tuning for mixture-of-expert model. *arXiv preprint arXiv:2411.08212*.

Niklas Muennighoff, Luca Soldaini, Dirk Groeneveld, Kyle Lo, Jacob Morrison, Sewon Min, Weijia Shi, Evan Pete Walsh, Oyvind Tafjord, Nathan Lambert, Yuling Gu, Shane Arora, Akshita Bhagia, Dustin Schwenk, David Wadden, Alexander Wetzig, Binyuan Hui, Tim Dettmers, Douwe Kiela, and 5 others. 2025. **OLMoE: Open mixture-of-experts language models**. In *The Thirteenth International Conference on Learning Representations*.

Noam Shazeer, \*Azalia Mirhoseini, \*Krzysztof Maziarz, Andy Davis, Quoc Le, Geoffrey Hinton, and Jeff Dean. 2017. **Outrageously large neural networks: The sparsely-gated mixture-of-experts layer**. In *International Conference on Learning Representations*.

Manxi Sun, Wei Liu, Jian Luan, Pengzhi Gao, and Bin Wang. 2024. **Mixture of diverse size experts**. In *Proceedings of the 2024 Conference on Empirical Methods in Natural Language Processing: Industry Track*, pages 1608–1621, Miami, Florida, US. Association for Computational Linguistics.

Mirac Suzgun, Nathan Scales, Nathanael Schärli, Sebastian Gehrmann, Yi Tay, Hyung Won Chung, Aakanksha Chowdhery, Quoc Le, Ed Chi, Denny Zhou, and 1 others. 2023. Challenging big-bench tasks and whether chain-of-thought can solve them. In *Findings of the Association for Computational Linguistics: ACL 2023*, pages 13003–13051.

Kimi Team, Angang Du, Bohong Yin, Bowei Xing, Bowen Qu, Bowen Wang, Cheng Chen, Chenlin Zhang, Chenzhuang Du, Chu Wei, and 1 others. 2025. Kimi-vl technical report. *arXiv preprint arXiv:2504.07491*.

An Wang, Xingwu Sun, Ruobing Xie, Shuaipeng Li, Jiaqi Zhu, Zhen Yang, Pinxue Zhao, Weidong Han, Zhanhui Kang, Di Wang, and 1 others. 2025. Hmoe: Heterogeneous mixture of experts for language modeling. In *Proceedings of the 2025 Conference on Empirical Methods in Natural Language Processing*, pages 21954–21968.

Zihan Wang, Deli Chen, Damai Dai, Runxin Xu, Zhuoshu Li, and Yu Wu. 2024. **Let the expert stick to his last: Expert-specialized fine-tuning for sparse architectural large language models**. In *Proceedings of the 2024 Conference on Empirical Methods in Natural Language Processing*, pages 784–801, Miami, Florida, USA. Association for Computational Linguistics.

An Yang, Anfeng Li, Baosong Yang, Beichen Zhang, Binyuan Hui, Bo Zheng, Bowen Yu, Chang Gao, Chengan Huang, Chenxu Lv, and 1 others. 2025. Qwen3 technical report. *arXiv preprint arXiv:2505.09388*.

Rowan Zellers, Ari Holtzman, Yonatan Bisk, Ali Farhadi, and Yejin Choi. 2019. Hellaswag: Can a machine really finish your sentence? *arXiv preprint arXiv:1905.07830*.

Qingru Zhang, Minshuo Chen, Alexander Bukharin, Pengcheng He, Yu Cheng, Weizhu Chen, and Tuo Zhao. 2023. **Adaptive budget allocation for parameter-efficient fine-tuning**. In *The Eleventh International Conference on Learning Representations*.

Jeffrey Zhou, Tianjian Lu, Swaroop Mishra, Siddhartha Brahma, Sujoy Basu, Yi Luan, Denny Zhou, and Le Hou. 2023. Instruction-following evaluation for large language models. *arXiv preprint arXiv:2311.07911*.

Yanqi Zhou, Tao Lei, Hanxiao Liu, Nan Du, Yanping Huang, Vincent Zhao, Andrew M Dai, Quoc V Le, James Laudon, and 1 others. 2022. Mixture-of-experts with expert choice routing. *Advances in Neural Information Processing Systems*, 35:7103–7114.

## A Experimental Details and Reproducibility

### A.1 Training Configurations

#### A.1.1 Model Configurations

**OLMoE-1B-7B:** 6.9B total parameters with 1.3B activated per forward pass. The model employs 16 layers with 64 experts per layer, activating the top-8 experts. Each expert has dimension 1024, with hidden size 2048.

**Phi-mini-MoE-instruct:** 7.6B total parameters with 2.4B activated per forward pass. The model employs 32 layers with 16 experts per layer, activating the top-2 experts. Each expert has dimension 960, with hidden size 4096.

#### A.1.2 Training Hyperparameters

Table 6 presents the complete hyperparameter settings for all experiments. All methods use AdamW optimizer with learning rate  $2 \times 10^{-5}$ , linear learning rate scheduler with 3% warmup, and weight decay 0.0. LoRA scaling factor  $\alpha$  is set to  $2 \times r$  for all configurations.

#### A.1.3 Growth Schedule and Router Training

**Growth window:** Rank growth begins after the learning rate warmup phase (3% of total steps: 1,140 steps for OLMoE, 570 steps for Phi) and continues until 200 steps before training completion. This ensures newly activated ranks receive

Hyperparameter	OLMoE	Phi
<i>Standard LoRA</i>		
Rank ( $r$ )	64	16
<i>DR-LoRA (ours)</i>		
Initial rank ( $r_{\text{init}}$ )	32	8
Maximum rank ( $r_{\text{max}}$ )	128	32
Target rank ( $r_{\text{target}}$ )	64	16
Growth interval ( $T_{\text{grow}}$ )	200	200
Module growth fraction ( $p_{\text{grow}}$ )	0.1	0.1
Usage EMA coefficient ( $\beta$ )	0.9	0.9
Rank penalty exponent ( $\gamma$ )	1.2	1.2
<i>Training configuration</i>		
Learning rate	$2 \times 10^{-5}$	
LR scheduler	Linear	
Warmup ratio	0.03	
Weight decay	0.0	
Optimizer	AdamW (fused)	
LoRA $\alpha$	$2 \times r$	
Epochs	1	1
Total steps	38,000	19,000
Micro-batch size	1	1
Gradient accumulation	4	8
Effective batch size	16	32
Max sequence length	4096	4096

Table 6: Complete hyperparameter settings for all experiments.

sufficient training. Growth occurs every 200 steps within this window.

**Layer synchronization:** All layers grow simultaneously at each growth event. The per-layer quota is computed as  $Q = \lceil N \times (r_{\text{target}} - r_{\text{init}}) / T_{\text{events}} \rceil$ , where  $N=128$  is the number of LoRA modules per layer (64 experts  $\times$  2 projections) and  $T_{\text{events}}$  is the number of scheduled growth events.

**Router training schedule:** The MoE router remains frozen during the warmup phase to stabilize LoRA training. After warmup, the router is unfrozen and trained jointly with LoRA modules until training completion. This allows the router to adapt to the evolved expert capabilities from dynamic rank allocation.

## A.2 Evaluation Protocol

### A.2.1 Benchmark Settings

All evaluations are conducted using the LM Evaluation Harness framework with vLLM backend (v1) for efficient inference. Table 7 summarizes the evaluation configuration for each benchmark.

**MMLU, BBH, GSM8k, IFEval, ARC-C, HellaSwag:** We use the LM Evaluation Harness with vLLM backend for efficient batch inference. Model outputs are generated using greedy decoding (temperature = 0.0) with automatic batch size selection based on GPU memory. All models are evaluated

Benchmark	Few-shot	Decoding	Split
MMLU	0-shot	Greedy	test
BBH	3-shot	Greedy	test
GSM8k	8-shot	Greedy	test
HumanEval	—	T=0.8	test
IFEval	0-shot	Greedy	test
ARC-C	25-shot	Greedy	test
HellaSwag	10-shot	Greedy	validation
MedQA	0-shot	Greedy	train
MedMCQA	0-shot	Greedy	validation
PubMedQA	0-shot	Greedy	train/test

Table 7: Evaluation settings for all benchmarks. All evaluations use greedy decoding (temperature = 0.0) except HumanEval which uses temperature 0.8 for sampling.

with chat template applied (for instruction-tuned models) and maximum model length set to 4096 tokens. BBH uses chain-of-thought prompting format. GSM8k employs 8-shot chain-of-thought prompting.

**HumanEval:** We evaluate code generation using pass@k metrics with  $k \in \{1, 10, 20\}$ . For each of the 164 programming problems, we generate  $n=20$  code samples using temperature 0.8 and max tokens 512. Following Chen (2021), we compute pass@k using the unbiased estimator:  $\text{pass@k} = \mathbb{E}_{\text{Problems}} \left[ 1 - \frac{\binom{n-c}{k}}{\binom{n}{k}} \right]$  where  $c$  is the number of correct samples among  $n$  total samples. We report mean and standard deviation across 3 independent runs with random seeds {42, 123, 456} to account for sampling variance.

**Medical benchmarks:** We construct training and evaluation datasets from three medical QA sources using a standardized chat format.

**MedQA:** US Medical Licensing Examination questions from GBaker/MedQA-USMLE-4-options. Questions are 4-option multiple choice. We use the train split as no official test split is available.

**MedMCQA:** Indian medical entrance exam questions from medmcqa dataset. We evaluate on the validation split. Questions are 4-option multiple choice with optional explanations.

**PubMedQA:** Biomedical literature QA from pubmed\_qa (pqa\_labeled subset). Questions require yes/no/maybe answers based on biomedical abstracts. We use available splits (train or test depending on dataset version).

All medical evaluations use greedy decoding with vLLM for fast inference. Answer extraction employs pattern matching to identify option letters

(A/B/C/D) or yes/no/maybe responses from model outputs. Evaluation uses maximum 20 new tokens as answers are typically single letters or words.

### A.2.2 Data Splits and Reproducibility

We use the standard test or validation splits provided by each benchmark through the LM Evaluation Harness and HuggingFace Datasets library. Specifically:

- MMLU, BBH, GSM8k, IFEval, ARC-C, HumanEval: Standard test splits
- HellaSwag: Validation split (as commonly used in the literature)
- Medical benchmarks: Train split for MedQA (no official test split), validation for MedMCQA, available splits for PubMedQA

We do not perform early stopping; all models train for exactly 1 epoch (38,000 steps for OLMoE, 19,000 steps for Phi). This ensures fair comparison across methods without tuning stopping criteria.

**Checkpoint evaluation:** We save model checkpoints every 6,000 steps during training and evaluate all intermediate checkpoints on the full benchmark suite. This allows us to track learning dynamics and verify stable convergence. Final results report performance at the last checkpoint.

**Multiple runs:** All experiments are conducted with 3 independent training runs using random seeds {42, 123, 456}.

## A.3 Computational Infrastructure

**Hardware:** All training experiments are conducted on a single server with  $4 \times$  NVIDIA L40S GPUs (48GB memory each).

**Distributed training:** We use DeepSpeed ZeRO-2 for distributed training with the following configuration:

- Mixed precision: bfloat16
- Gradient communication: overlap enabled
- Contiguous gradients: enabled
- Reduce bucket size: auto

### Optimization features:

- Flash Attention 2 (version 2.8.3) for memory-efficient attention computation
- Gradient checkpointing enabled to reduce memory consumption

- Fused AdamW optimizer for improved training speed

**Training time:** Complete training times for 1 epoch are reported in Table 8.

Method	OLMoE	Phi
LoRA ( $r=64$ )	39.7 hours	—
LoRA ( $r=128$ )	42.4 hours	—
LoRA ( $r=16$ )	—	30.2 hours
DR-LoRA (ours)	43.2 hours	32.7 hours

Table 8: Wall-clock training time for 1 complete epoch on  $4 \times$  L40S GPUs.

## A.4 Dataset Details

### A.4.1 OLMoE SFT Mix

OLMoE SFT Mix dataset combines the following sources with specified mixture weights:

- allenai/tulu-v2-sft-mixture-olmo-4096 (weight: 1.0)
- HuggingFaceH4/no\_robots (weight: 1.0)
- meta-math/MetaMathQA (weight: 0.25)
- m-a-p/CodeFeedback-Filtered-Instruction (weight: 1.0)
- ai2-adapt-dev/daring-anteater-specialized (weight: 1.0)

The dataset emphasizes diverse instruction-following capabilities including general conversation, mathematical reasoning, and code generation.

### A.4.2 Medical QA Dataset

For Phi experiments on medical domain adaptation, we construct a specialized dataset combining three medical QA sources to create a diverse medical instruction-following corpus:

- **MedQA:** US Medical Licensing Examination questions from bigbio/med\_qa (en\_bigbio\_qa config, train split). Questions are 4-option multiple choice extracted from USMLE practice exams covering clinical knowledge, diagnosis, and treatment.
- **MedMCQA:** Indian medical entrance exam questions from medmcqa (train split). Questions span anatomy, physiology, pharmacology, and clinical medicine with 4 options and optional explanations.

- **PubMedQA:** Biomedical literature QA from `pubmed_qa` (`pqa_labeled` subset, train split). Questions derived from PubMed abstracts requiring yes/no/maybe answers with scientific explanations.

**Dataset construction:** Each source is converted to a standardized chat format with user/assistant message pairs. For multiple-choice questions (MedQA, MedMCQA), the prompt includes the question and options labeled A-D, with the response providing the correct answer letter and explanation. For PubMedQA, the prompt includes the biomedical context (truncated to 1200 characters if needed) and question, with yes/no/maybe responses and explanations. All datasets are combined and shuffled with seed 42 before training. This medical dataset tests DR-LoRA’s ability to allocate capacity for domain-specific adaptation beyond general instruction following, particularly whether the method can identify and expand high-utility experts for specialized knowledge.

## B Computational Cost Analysis

### B.1 Memory Analysis

We empirically measure the GPU memory overhead introduced by DR-LoRA’s rank reservation strategy. Under our experimental configuration, we observe that standard LoRA ( $r = 64$ ) consumes approximately 40 GB per GPU, while DR-LoRA ( $r_{\max} = 128$ ,  $r_{\text{init}} = 32$ ,  $r_{\text{avg}} = 64$  at convergence) requires approximately 43 GB per GPU, resulting in a 3 GB overhead (approximately 7.5% increase).

This overhead consists of two components: (1) The **static overhead** of approximately 1.2 GB per GPU stems from allocating full parameter space for  $r_{\max} = 128$  ranks while activating only  $r_{\text{avg}} = 64$  on average. Under DeepSpeed ZeRO-2, parameters (bf16) are replicated across devices, contributing 538 MB, while gradients (bf16) and optimizer states (fp32) are sharded across 4 GPUs, contributing 134 MB and 538 MB respectively. (2) The **dynamic overhead** of approximately 1.8 GB per GPU arises from a deliberate design choice in our forward pass computation. While masking could be applied *before* matrix multiplication to minimize activation memory, we implement masking *after* multiplication for two key reasons. First, pre-masking requires dynamic tensor indexing (e.g.,  $A[\text{mask}, :]$ ), which introduces irregular memory access patterns and prevents efficient GPU

kernel fusion. Our post-multiplication approach enables standard GEMM operations that fully utilize tensor cores, maintaining computational efficiency. Second, this design integrates seamlessly with PyTorch’s autograd and mixed-precision training, avoiding custom CUDA kernels while maintaining numerical stability.

This design choice means forward activations are computed at full  $r_{\max}$  dimensionality before selective masking in the backward pass. With gradient checkpointing enabled, intermediate activations across gradient accumulation steps, backward gradient buffers, and hook mechanisms for importance tracking collectively contribute to the dynamic overhead, along with memory fragmentation and framework-level bookkeeping inherent to distributed training systems.

The 1.8 GB dynamic overhead represents 4.5% of total GPU memory and constitutes a deliberate trade-off that eliminates computational bottlenecks from dynamic masking while remaining well within typical GPU budgets. This design enables DR-LoRA to maintain competitive training speed (see §B.2) while achieving substantial performance gains. For extremely memory-constrained scenarios, practitioners can implement pre-masking strategies at the cost of increased training time, or reduce  $r_{\max}$  to  $1.5 \times r_{\text{target}}$  to lower the overhead.

### B.2 Training Time Analysis

We measure wall-clock training time for one complete epoch on the OLMoE SFT Mix dataset using 4×L40S GPUs. As shown in Table 9, standard LoRA with  $r = 64$  completes training in 39.7 hours, while increasing rank to  $r = 128$  extends training time to 42.4 hours (1.07× baseline). DR-LoRA, starting from  $r_{\text{init}} = 32$  and growing to  $r_{\text{avg}} = 64$ , requires 43.2 hours (1.09× baseline), achieving a final performance of 42.6 points compared to 40.8 for  $r = 64$  and 41.3 for  $r = 128$ .

Method	Time	Rel.	Rank	Perf.
LoRA ( $r=64$ )	39.7h	1.00×	64	40.8
LoRA ( $r=128$ )	42.4h	1.07×	128	41.3
DR-LoRA	43.2h	1.09×	32→64	<b>42.6</b>

Table 9: Wall-clock training time comparison.

DR-LoRA incurs a modest 9% training time overhead compared to standard LoRA ( $r = 64$ ), which is comparable to simply using  $r = 128$  (7% overhead). This near-equivalence directly reflects

our design decision to prioritize computational efficiency through post-multiplication masking, as discussed in the memory overhead analysis. The additional 2 percentage points of overhead in DR-LoRA represent the computational cost of dynamic rank allocation mechanisms, including importance scoring, expert usage tracking, and periodic rank growth, which are absent in static LoRA.

### B.3 FLOPs Analysis

We analyze the computational cost of DR-LoRA in terms of floating-point operations (FLOPs) during training. The total FLOPs consist of base expert computation and LoRA adaptation.

For a single forward pass, base expert FLOPs are:

$$\text{FLOPs}_{\text{base}} = 4BLK \cdot d_m \cdot d_e \quad (13)$$

where  $B=4096$  is the effective batch size,  $L=16$  is the number of layers,  $K=8$  is the number of activated experts per layer,  $d_m=2048$  is the hidden dimension, and  $d_e=1024$  is the expert dimension. LoRA adds:

$$\text{FLOPs}_{\text{LoRA}} = 8BLK \cdot d_e \cdot r \quad (14)$$

where  $r$  is the LoRA rank and each expert has two LoRA modules (up\_proj and down\_proj).

**Rank Evolution During Training.** Table 10 shows how DR-LoRA’s average rank evolves during training. Starting from  $r_{\text{init}} = 32$ , the rank progressively grows through our dynamic allocation mechanism, reaching the target average of  $r = 64$  by step 37,800. The weighted average rank across the entire training process is 48.12, substantially lower than both LoRA ( $r = 64$ ) and LoRA ( $r = 128$ ).

Step	Avg Rank	Progress	Total Ranks
0	32.00	50.0%	65,536
6,000	36.49	57.0%	74,736
12,000	41.88	65.4%	85,776
18,000	47.27	73.9%	96,816
24,000	52.66	82.3%	107,856
30,000	58.05	90.7%	118,896
37,800	64.00	100.0%	131,072
Weighted average: 48.12			

Table 10: Evolution of DR-LoRA’s average rank during training (37,997 total steps). Progress indicates percentage toward target  $r = 64$ .

**FLOPs Comparison.** Table 11 presents the FLOPs analysis for different methods. DR-LoRA has identical LoRA FLOPs to LoRA ( $r = 128$ ). However, since base expert computation dominates total FLOPs (94%), the overall increase is only 5.9% compared to LoRA ( $r = 64$ ), closely matching the observed 6.8% training time increase.

Method	Base	LoRA	Total	Rel.
No LoRA	4398.0	—	4398.0	1.000 $\times$
LoRA ( $r=64$ )	4398.0	274.9	4672.9	1.062 $\times$
LoRA ( $r=128$ )	4398.0	549.8	4947.8	1.125 $\times$
DR-LoRA	4398.0	549.8	4947.8	1.125 $\times$

Table 11: FLOPs per sample (GFLOPs) for forward pass. Base expert computation dominates (94%), making LoRA’s contribution relatively small (6–11%).

### B.3.1 Training Time vs. FLOPs Correlation

Our wall-clock training time measurements (Table 9) align closely with FLOPs analysis. LoRA ( $r = 128$ ) incurs +6.8% training time with +5.9% total FLOPs, demonstrating strong correlation. DR-LoRA shows +8.8% training time with identical FLOPs to LoRA ( $r = 128$ ), where the additional 2 percentage points represent computational overhead from dynamic rank allocation mechanisms (importance scoring, expert usage tracking, and periodic rank growth).

## C Additional Experimental Results

### C.1 Expert Rank Evolution Visualization

To illustrate how DR-LoRA dynamically constructs heterogeneous rank distributions, we visualize the evolution of expert LoRA ranks throughout training in Figure 5. At the early stage (Epoch 0.16), most experts remain at the initial rank  $r_{\text{init}} = 32$  (shown in yellow), with only a few high-saliency experts receiving additional capacity (darker colors). By mid-training (Epoch 0.47), a clear heterogeneous pattern emerges as DR-LoRA progressively allocates ranks to task-relevant experts based on routing frequency and learning intensity. At the final stage (Epoch 1.0), the rank distribution becomes highly differentiated, with some experts reaching the maximum rank  $r_{\text{max}} = 128$  (dark red) while others remain at lower ranks, reflecting their varying importance to the target task. This progression demonstrates DR-LoRA’s ability to automatically discover and amplify task-relevant experts through dynamic capacity allocation, forming a

Rank Alloc. Strategy	GSM8k	HE	IF	Avg
Global	30.7	36.5	29.3	32.2
<b>Per-Layer</b>	32.8	39.1	32.7	34.9

Table 12: Per-layer vs. global rank allocation.

task-adaptive structure without manual intervention.

## C.2 Per-Layer vs. Global Rank Allocation

We compare two rank allocation strategies: distributing the parameter budget globally across all layers versus independently within each layer.

Figure 6(a) shows that expert saliency scores vary systematically across layers, with deeper layers exhibiting up to  $6.12 \times$  higher average saliency due to gradient flow and abstract representations. Under global allocation, high-saliency deep-layer experts dominate rank allocation, causing resource concentration. Figure 6(b) quantifies this imbalance: while per-layer allocation maintains uniform distribution (exactly 8,192 ranks per layer), global allocation ranges from 6,480 to 9,072 ranks (31.6% deviation), under-provisioning shallow layers and over-provisioning deep layers.

Table 12 shows per-layer allocation outperforms global allocation by +2.7 average points, validating that preventing resource concentration enables more effective adaptation. All DR-LoRA results use per-layer allocation.

## C.3 Comparison with Same-Rank LoRA

To isolate the impact of dynamic rank allocation from simply having more parameter capacity, we compare DR-LoRA against standard LoRA with matched maximum rank. Specifically, we train standard LoRA with  $r = 128$  (matching DR-LoRA’s  $r_{\max} = 128$ ) on OLMoE using the OLMoE SFT Mix dataset, while DR-LoRA grows from  $r_{\text{init}} = 32$  to average  $r_{\text{target}} = 64$ .

Table 13 presents the results. Despite having only half the average active parameters (64 vs. 128), DR-LoRA outperforms the fixed  $r = 128$  baseline by +1.3 average points (42.6 vs. 41.3). This demonstrates that DR-LoRA’s performance gains stem from *intelligent parameter allocation* rather than simply having more parameters. The dynamic allocation mechanism successfully identifies and prioritizes task-relevant experts, achieving superior adaptation with substantially fewer active parameters.

From a computational perspective, DR-LoRA and LoRA ( $r = 128$ ) have comparable training costs (43.2 h vs. 42.4 h, as shown in Table 9), but DR-LoRA achieves significantly better performance. By accepting  $r = 128$ -equivalent computational cost, DR-LoRA achieves  $3.6 \times$  better performance improvement than LoRA ( $r = 128$ ): +1.8 points versus +0.6 points above the  $r = 64$  baseline. This shows that *where* parameters are allocated matters substantially more than *how many* parameters are allocated.

Method	Avg Rank (Max)	MMLU	HellaSwag	BBH	GSM8k	ARC-C	HumanEval	IFEval	Avg
Base	–	<b>50.5</b>	<b>59.2</b>	32.3	6.1	<b>54.2</b>	22.1	16.5	34.4
LoRA	64 (64)	50.3	55.9	<b>34.5</b>	30.2	51.9	34.1	28.8	40.8
LoRA	128 (128)	49.3	55.8	34.0	32.0	52.0	35.5	30.7	41.3
DR-LoRA	64 (128)	50.0	55.9	<b>34.5</b>	<b>32.8</b>	53.2	<b>39.1</b>	<b>32.7</b>	<b>42.6</b>

Table 13: Performance comparison between DR-LoRA and same-rank LoRA on OLMoE. Despite having only half the average active parameters as LoRA with  $r = 128$ , DR-LoRA achieves superior performance through intelligent dynamic allocation. Bold indicates best performance.

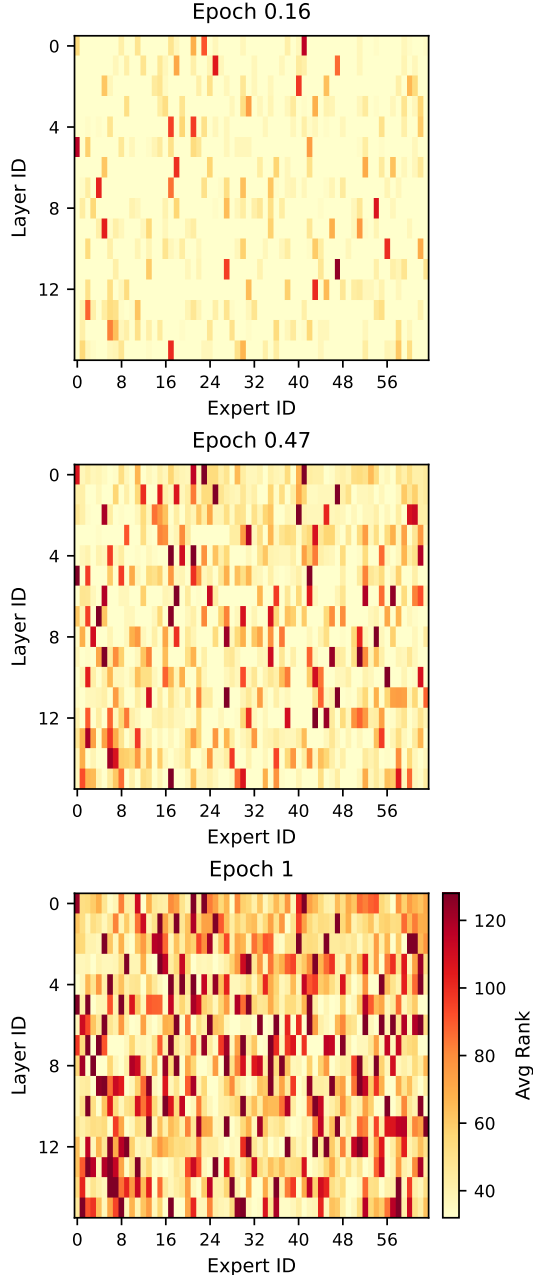


Figure 5: Evolution of expert LoRA ranks during DR-LoRA training on OLMoE. Each heatmap shows the average rank per expert (averaged over `up_proj` and `down_proj`) at different training stages, with high-rank experts (darker red) concentrated in task-relevant positions.

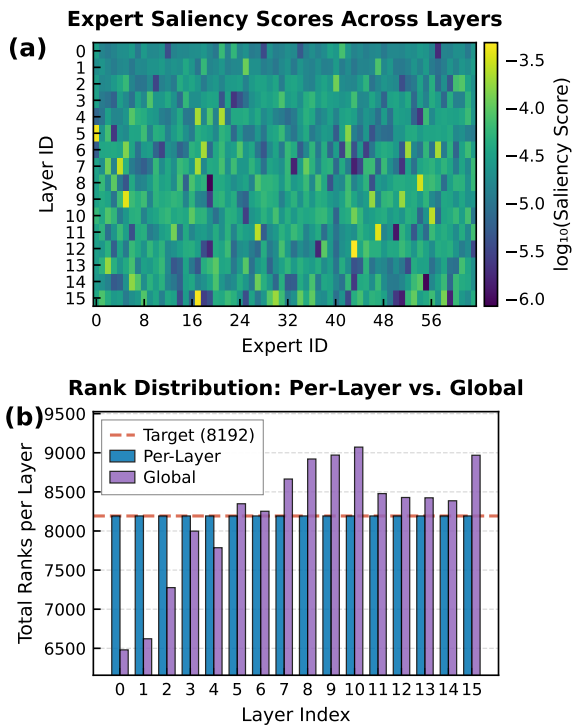


Figure 6: Analysis of per-layer vs. global rank allocation strategies. (a) Expert saliency scores show systematic layer-wise heterogeneity, with deeper layers exhibiting substantially higher average saliency. (b) Under global allocation, this heterogeneity causes rank monopolization: deep layers receive up to +10.7% excess ranks while shallow layers suffer up to -20.9% under-provisioning, leading to inferior performance. Per-layer allocation prevents this imbalance by ensuring uniform allocation across layers.

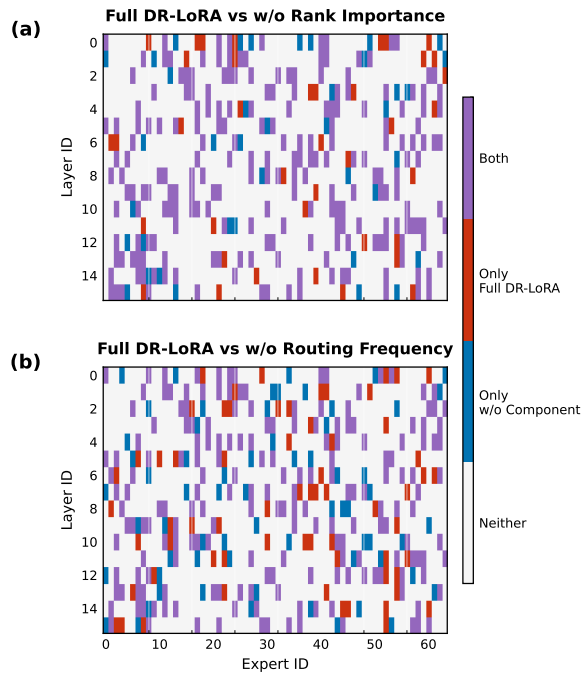


Figure 7: Expert rank allocation comparison between full DR-LoRA and ablated variants. **Top:** Overlap with the variant without rank importance (using only routing frequency  $f_{\ell,i}$ ). **Bottom:** Overlap with the variant without routing frequency (using only rank importance  $g_{\ell,i}$ ). Each heatmap shows the top-25% highest-ranked experts (16 out of 64 per layer) across all layers.